ENOC 2011, 24-29 July 2011, Rome, Italy

Dynamics of Coupled Microbubbles with Large Fluid-Compressibility Delays

Christoffer Heckman, Richard Rand
Department of Mechanical and Aerospace Engineering, Cornell University, Ithaca, New York, USA

Summary. The theory of differential delay equations is applied to analyze a system of two bubbles related via a delayed coupling term. The dynamics of the system are described by perturbation analyses and bifurcations are detected via continuation using DDE-BIFTOOL. It is shown that for these delays, synchronized oscillation and quasiperiodic motions exist for the coupled system.

Motivation

Microbubbles have been a topic of research for almost a century, with contemporary research focused on potential applications of bubbles for biomedical purposes such as ultrasound imaging. Other work has analyzed single bubbles under the influence of an ultrasound driver, revealing the existence of a chaotic attractor for naturally realized parameter values[1]. The present study is concerned with the behavior of two bubbles as a system of coupled oscillators with interactions depending on the delayed state of each bubble. The study therefore has applications in the broader theory of differential delay equations (DDEs).

Equations of motion

Central to this study is the equation that governs the radial dynamics of a gas-filled bubble in a fluid. This equation is known as the Rayleigh-Plesset Equation; the form used in our analysis was derived by Keller et al. [2] using the wave equation on potential functions for the fluid velocity.
The radius of a bubble submerged in a fluid is inversely related to the pressure in the fluid. If the radius is changing with time, it sends pressure waves through the compressible fluid, which may then affect the radial dynamics of surrounding bubbles. This transit time gives rise to a time delay in the coupled bubble dynamics. The equations of motion for the coupled system are shown in eq. (1).
To analyze this system, we restrict our study to the in-phase manifold (IPM) for which the dynamics of the two bubbles are identical, i.e. $a = b$, $\dot{a} = \dot{b}$. This distills (1) into a single nonlinear two-degree of freedom DDE.

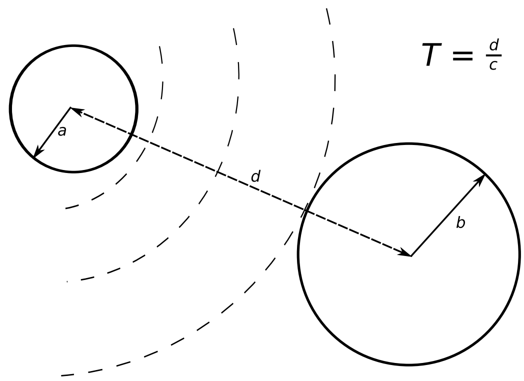

Figure 1: Two microbubbles in a fluid with sound speed c separated by a distance d, giving rise to a time delay for acoustic waves $t = d/c$.

$$(\dot{a} - c)\left(a\ddot{a} + \frac{3}{2}\dot{a}^2 - a^{-3\gamma} + 1\right) - \dot{a}^3 - (3\gamma - 2)\, a^{-3\gamma}\dot{a} - 2\dot{a} = P\dot{b}(t - T)$$
$$\left(\dot{b} - c\right)\left(b\ddot{b} + \frac{3}{2}\dot{b}^2 - b^{-3\gamma} + 1\right) - \dot{b}^3 - (3\gamma - 2)\, b^{-3\gamma}\dot{b} - 2\dot{b} = P\dot{a}(t - T) \tag{1}$$

Dynamics on the in-phase manifold

On the in-phase manifold, (1) has an equilibrium solution of $a = 1$ which we refer to as the "in-phase mode." Rewriting (1) by substituting $a = 1 + x$ to track deviations x from the equilibrium point and linearizing about $x = 0$ gives

$$c\ddot{x} + 3\gamma\dot{x} + 3c\gamma x = P\dot{x}\,(t - T) \tag{2}$$

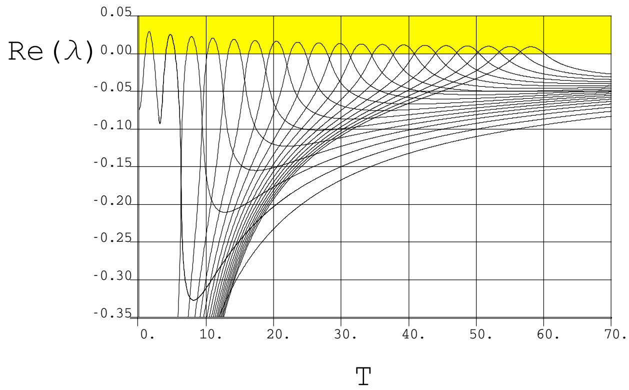

Figure 2: Locus of $\Re(\lambda)$ vs. T.

This equation has solutions $x = \exp(\lambda t)$. Substituting this solution into (2) yields a characteristic equation on λ with an infinite number of roots. To determine stability of the equilibrium point, we identify whether any of these roots are on the right-half of the complex plane. If so, the equilibrium point is unstable; otherwise, it is stable.
Using AUTO, we may track the real and imaginary parts of each root of (2) as T varies. Fig. 2 shows how the real part of several roots close to the imaginary axis behave—note that for regions of T where a root has $\Re(\lambda) > 0$, the in-phase mode is unstable. To calculate these roots, we specify representative parameter values $\gamma = \frac{4}{3}$, $P = 10$, and $c = 94$.

By setting $\lambda = i\omega_{cr}$, one may calculate pairs of solutions (ω_{cr}, T_{cr}) corresponding to when the equilibrium point has neutral stability. We find that while only two values of ω_{cr} solve the equation (henceforth called ω_α and ω_β), there are two "kinds" of T_{cr} solving (2). The bifurcation points in T are

$$T_\alpha = \frac{\arccos(-.4) + 2\pi n}{\omega_\alpha}\ (n \in \mathbb{Z})\ , T_\beta = \frac{-\arccos(-.4) + 2\pi m}{\omega_\beta}\ (m \in \mathbb{Z})$$

These changes in stability correspond to Hopf bifurcations, and periodic solutions split from the in-phase mode in the form of limit cycles. These limit cycles have been analyzed using Lindstedt's method [3].

Sequence of Hopf bifurcations

All T_α Hopfs are associated with eigenvalues crossing into the right-half of the complex plane, whereas all T_β Hopfs have a pair of roots returning to the left-half plane. Thus, T_α is associated with supercritical Hopf bifurcation, and T_β with subcritical Hopf bifurcation.
Using numerical integration and continuation in DDE-BIFTOOL, the bifurcation diagram for the system for very delays large may be drawn. For $0 < T < 40$, Fig. 3 illustrates typical bifurcating sequences with increasing T.

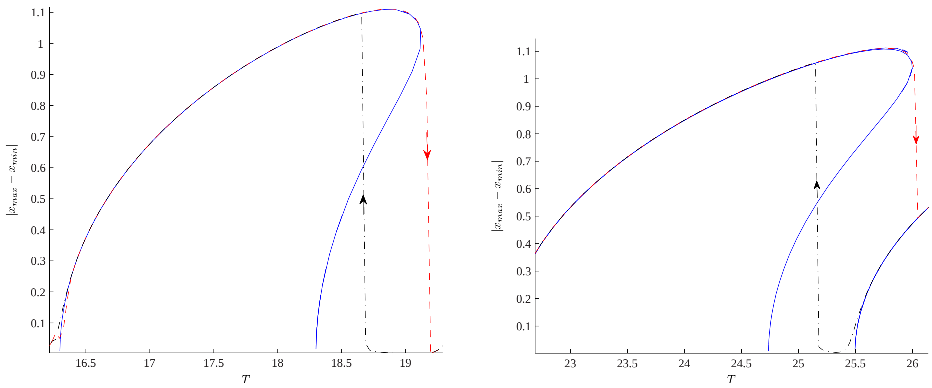

Figure 3: Profiles of bifurcating limit cycles for regions of T with distinctly different dynamics. Note that the solid blue curves are continuation, dashed red curves are integration with increasing T, and dot-dashed black curves are integration with decreasing T.

For large enough T, a β-Hopf precedes an α-Hopf
The countable infinity of Hopf bifurcations is not evenly spread. Using the previously specified parameters, $\omega_\alpha \approx 2.0493$ and $\omega_\beta \approx 1.9518$; this means that for some n, m there will be a subsequence of two β-Hopfs without an α-Hopf between them. In the neighborhood of this switching, quasiperiodic solutions and periodic solutions coexist. Figure 4 provides a bifurcation diagram of this region, as well as a time series of the quasiperiodic solutions. It is suspected that this quasiperiodic behavior is connected with the unfolding of a Hopf-Hopf bifurcation, corresponding to a four-dimensional center manifold and in the neighborhood of which torus bifurcations are present, see [4].

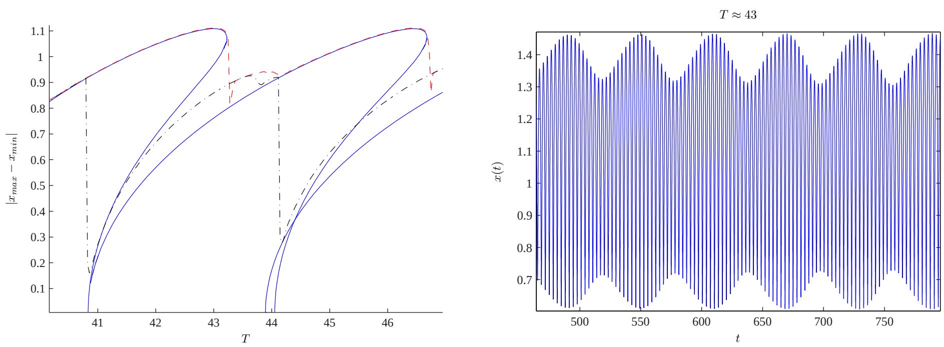

Figure 4: Behavior of the in-phase mode in the third region. Numerical integration tracks the quasiperiodic behavior, whereas continuation shows the persistence of periodic solutions.

References

[1] Parlitz U., Englisch V., Scheffczyk C., Lauterborn W. (1990) Bifurcation structure of bubble oscillators. *J. Acoust. Soc. Am.* **88** (2):1061–1077.

[2] Keller J., Kolodner I. (1956) Damping of Underwater Explosion Bubble Oscillations *J. App. Phys.* **27** (10): 1152–1161.

[3] Heckman C.R., Sah S.M., Rand R.H. (2010) Dynamics of microbubble oscillators with delay coupling *Commun Nonlinear Sci Numer Simulat* **15**:2735–2743.

[4] Guckenheimer J., Kuznetsov Y.A. (2008) Hopf-Hopf bifurcation. Scholarpedia, 3(8):1856.